HHS Public Access

Author manuscript

Mol Psychiatry. Author manuscript; available in PMC 2021 October 13.

Published in final edited form as:

Mol Psychiatry. 2021 July ; 26(7): 3152–3168. doi:10.1038/s41380-020-00921-1.

Cocaine-Induced Neural Adaptations in the Lateral Hypothalamic Melanin-Concentrating Hormone Neurons and the Role in Regulating Rapid Eye Movement Sleep After Withdrawal

Yao Wang[1,2,*], **Rong Guo**[1,*], **Bo Chen**[1,#], **Tanbin Rahman**[3,##], **Li Cai**[1], **Yizhi Li**[1,2], **Yan Dong**[1,2], **George C. Tseng**[3], **Jidong Fang**[4], **Marianne L. Seney**[1], **Yanhua H. Huang**[1]

[1]Department of Psychiatry, University of Pittsburgh, Pittsburgh, PA

[2]Department of Neuroscience, University of Pittsburgh, Pittsburgh, PA

[3]Department of Biostatistics, University of Pittsburgh, Pittsburgh, PA

[4]Department of Psychiatry and Behavioral Health, Penn State College of Medicine, Hershey, PA

Abstract

Sleep abnormalities are often a prominent contributor to withdrawal symptoms following chronic drug use. Notably, rapid eye movement (REM) sleep regulates emotional memory, and persistent REM sleep impairment after cocaine withdrawal negatively impacts relapse-like behaviors in rats. However, it is not understood how cocaine experience may alter REM sleep regulatory machinery, and what may serve to improve REM sleep after withdrawal. Here, we focus on the melanin-concentrating hormone (MCH) neurons in the lateral hypothalamus (LH), which regulate REM sleep initiation and maintenance. Using adult male Sprague Dawley rats trained to self-administer intravenous cocaine, we did transcriptome profiling of LH MCH neurons after long-term withdrawal using RNA-sequencing, and performed functional assessment using slice electrophysiology. We found that three weeks after withdrawal from cocaine, LH MCH neurons exhibit a wide range of gene expression changes tapping into cell membrane signaling, intracellular signaling, and transcriptional regulations. Functionally, they show reduced membrane excitability and decreased glutamatergic receptor activity, consistent with increased expression of voltage-gated potassium channel gene *Kcna1* and decreased expression of metabotropic glutamate receptor gene *Grm5*. Finally, chemogenetic or optogenetic stimulations of LH MCH neural activity increase REM sleep after long-term withdrawal with important differences. Whereas chemogenetic stimulation promotes both wakefulness and REM sleep, optogenetic

Corresponding Author: Dr. Y.H. Huang, Corresponding Address: 450 Technology Dr., Pittsburgh, PA 15219, yhhuang@pitt.edu, Phone: 412-624-7581.

[#]Current Address: Shenzhen Key Laboratory of Drug Addiction, CAS Key Laboratory of Brain Connectome and Manipulation, the Brain Cognition and Brain Disease Institute, Shenzhen Institutes of Advanced Technology, Chinese Academy of Sciences; Shenzhen-Hong Kong Institute of Brain Science-Shenzhen Fundamental Research Institutes, Shenzhen, China

[##]Current Address: Department of Biostatistics, University of Texas MD Anderson Cancer Center, Houston, TX

[*]These authors contributed equally to this work

Disclosure: Dr. Jidong Fang is the creator of SleepMaster software, and the owner of Biosoft Studio. All other authors declare no conflict of interest. The content is solely the responsibility of the authors and does not necessarily represent the official views of the National Institutes of Health.

stimulation of these neurons in sleep selectively promotes REM sleep. In summary, cocaine exposure persistently alters gene expression profiles and electrophysiological properties of LH MCH neurons. Counteracting cocaine-induced hypoactivity of these neurons selectively in sleep enhances REM sleep quality and quantity after long-term withdrawal.

Keywords

cocaine; REM sleep; MCH neurons; electrophysiology; RNAseq

Introduction

Sleep abnormalities often accompany withdrawal from chronic use of a variety of drugs, including cocaine, opioid, cannabis, and nicotine[1, 2]. Chronic cocaine users often experience reduced total sleep time and increased sleep fragmentation resembling chronic insomnia[1, 3–5], which have been recapitulated in the rat cocaine self-administration model[6]. The persistent sleep problems are not only a comorbidity but may drive the vicious cycle by fostering drug use and relapse[6–12]. In particular, rapid eye movement (REM) sleep regulates the formation and modulation of emotional memories[13–18], and cocaine-induced long-term REM sleep impairment negatively impacts relapse-like behaviors in rats after withdrawal[6]. However, it is not understood whether and how cocaine experience imposes persistent changes to REM sleep regulatory machinery, and what may serve as effective means to improve REM sleep after withdrawal.

Melanin-concentrating hormone (MCH)-producing neurons are mainly located in the lateral hypothalamus and the nearby zona incerta (LH for short)[19]. They are broadly connected to functionally diverse brain regions, including those that regulate sleep, mood, memory, or reward motivation[20–25]. They respond to a variety of neurotransmitters, modulators, and small molecules through expression of diverse membrane receptors[26–29]. MCH neural activity is predominantly observed during REM sleep, some during feeding and certain explorative behaviors, and are otherwise quiescent[30, 31]. MCH signaling as well as MCH neural activity promote REM sleep[22, 32–34], and they respond to REM sleep deprivation as part of the homeostatic regulatory mechanisms[35–37]. Repeated cocaine exposure and withdrawal induces persistent decrease in REM sleep and increase in fragmentation[1, 3, 5, 6], however, it is not understood whether and how MCH neurons may be affected following cocaine experience and withdrawal. Here, we combine transcriptome profiling and *in vitro* slice electrophysiology to identify cocaine-induced long-term changes in LH MCH neurons, and utilize chemogenetic and optogenetic approaches to examine whether and how interventions of MCH neural activity may improve REM sleep after long-term withdrawal from cocaine.

Materials and Methods

Subjects

Male Sprague-Dawley rats (Harlan, MD) at postnatal day 28–42 at the beginning of the experiments were used. Rats were singly housed under a 12-h reverse light/dark cycle (off

at 7:00, on at 19:00). Temperature (22 ± 1°C) and humidity (60 ± 5%) were controlled. The rats were used in all experiments in accordance with protocols approved by the Institutional Animal Care and Use Committees at University of Pittsburgh.

Viral vectors

AAV5-MCHp-GFP and AAV5-MCHp-ChR2-EYFP constructs were kindly provided by Dr. Priyattam J. Shiromani. AAV5-MCHp-DREADDs(Gq)-mCherry was constructed by piecing together MCHp and hm3D(Gq)-mCherry (Addgene #50478). All viral vectors were packaged at University of North Carolina Vector Core (5.8×10^{12} vg/ml; 3.2×10^{12} vg/ml; 1.1×10^{13} vg/ml).

Surgeries

Cocaine self-administration surgery, EEG/EMG surgery, and stereotaxic injections of viral vectors were similar to previously described[6, 38–42], and combined per experimental designs. Rats were anesthetized using ketamine (Henry Schein)/xylazine (100/10 mg/kg, SC.) and placed in a stereotaxic apparatus (Kopf Instruments). For viral vector injections, a 34-gauge injection needle connected to a Hamilton syringe driven by a microinfusion pump (Harvard Apparatus) was used to bilaterally inject 1.0 μl/site (0.1 μl/min) of the viral vector solution into the LH and zona incerta (in mm): AP −2.56, ML +/−0.9, DV −8.1. For *in vivo* optogenetic studies, optic fibers (200-μm core) with flat tips were bilaterally implanted directly above the LH zona incerta area (AP −2.56, ML +/−1.2, DV −7.5). For EEG/EMG surgery, two stainless-steel wire EMG electrodes (E363/76/10mm, Plastics One, Roanoke, VA) were inserted into the nuchal neck muscle and two pairs of screw-mounted wire EEG electrodes (E363/20/2.4/15mm, Plastics One) were installed contralaterally through the skull over the parietal and frontal cortices (AP +5, ML +/−2; AP −5, ML +/−5). The head implants were fixed to the skull with light-cure dental composite (Prime-Dent flowable visible light cure composite, Prime Dental Manufacturing Inc., Chicago, IL). All rats were single-housed post-surgery and during subsequent experimentation. Rats started behavioral training 1–2 weeks after surgery.

Imaging of viral-mediated gene expression

Tissue preparation and imaging procedures were similar as described previously[40, 43]. Rabbit anti-MCH (H-070–47, Phoenix Pharmaceuticals) was diluted at 1:000, and secondary antibodies (Alexa Fluor 488-conjugated donkey anti-rabbit IgG, AB150073, Abcam; Alexa Fluor 594-conjugated donkey anti-rabbit IgG, AB150076, Abcam) were used at 1:500 each. Fluorescence images were taken under an Olympus IX71 fluorescence microscope at 4× or 10× original magnification, using QImaging camera and MetaMorph Advanced software.

Cocaine self-administration

Cocaine self-administration training was similar as described previously[6]. It was conducted during the dark phase in operant-conditioning chambers (Med Associates, VT), containing nose-poke holes with conditioned stimulus (CS) light, house light, and cocaine-infusion line. Rats were trained using a fixed ratio (FR) 1 reinforcement schedule (0.75 mg/kg over 6 sec per infusion, 20 sec time-out). Nose-pokes in the inactive hole had no reinforcement

consequences but were recorded. Rats with saline self-administration training were used as controls (Figs 1,2). Rats that received at least 20 cocaine infusions during the overnight session were subject to a subsequent 5-day training (2 hrs daily). Cocaine HCl (provided by NIDA Drug Supply Program) was dissolved in 0.9% NaCl saline.

Laser Microdissection

Tissue preparation was according to established methods[44, 45]. Briefly, the brain was fresh-frozen and cryosectioned into 20 μm coronal sections that contained LH GFP-labeled MCH neurons. The sections were thaw-mounted onto polyethylene napthalate membrane-coated slides (Leica Microsystems; #11505158; Bannockburn, IL, USA) that had been pre-treated with UV light at 254 nm for 30 min.

After complete dehydration through serial ethanol solutions (75% for 2 seconds, 95% for 10 seconds, 100% for 10 seconds x 2 times), laser microdissection was performed using a Leica LMD6500 system under 40x objective with the guidance of GFP fluorescence. 150 GFP-labeled neurons within the LH/zona incerta region were collected from each rat. Cells were collected into 0.5 ml microtubes (Ambion, Foster City, CA, USA) and lysed in 150 μl of RLT Buffer Plus (Qiagen, Valencia, CA, USA) with 30 sec-vortexing less than 3 hrs after collection, and stored at −80 °C until further processing.

RNA extraction and RNA-sequencing

Total RNA was extracted using the RNeasy Plus Micro Kit (Qiagen Cat. No. 74034) according to the manufacturer's instructions. RNA integrity was measured using the Agilent RNA 6000 Pico Kit on an Agilent 2100 Bioanalyzer. Samples with RNA integrity number (RIN) of higher than 7 were considered suitable for RNA-sequencing, which was performed using Illumina NextSeq 500 by the University of Pittsburgh Health Sciences Sequencing Core at Children's Hospital of Pittsburgh. cDNA was produced using the SMARTer Ultra Low input RNA kit (Clontech Laboratories, Inc). Paired-end sequencing was performed (2 × 75 bp reads). Average sample coverage was 32.76 million reads before alignment. Per base sequence quality was high (Phred score > 31 for all samples), indicating good quality of the experimental data.

Gene expression profiling

Reference genome for rat and the corresponding annotation files are obtained from Ensembl. The alignment rate was about ~85% for each sample, and 48,610 unique genes were identified. Genes were retained for further analysis if counts per million (CPM) were greater than 1 in 75% or more subjects. After filtering, 15,585 genes remained and were used for differential expression (DE) analysis by applying the DEseq2 package[46]. 454 genes showing significant differences ($p<0.05$; >1.2-fold cutoff) in expression from saline vs. cocaine-treated rats were analyzed using Database for Annotation, Visualization and Integrated Discovery (DAVID) webtool to identify enriched functional gene ontology (GO). We used this strategy to determine if specific biological processes (BP) were the target of cocaine-induced transcriptional alterations in LH MCH neurons. For Supplementary Tables 1,2, gene names and information on the presumed functions were obtained from https://www.genecards.org.

Slice electrophysiology

Acute NAc or LH slice preparation and electrophysiological recordings were similar as described previously[40, 47, 48]. Recording temperature was maintained at 31 ± 1°C. Loose-patch recordings were made at $V_m = 0$ using electrodes of 3 – 5 MΩ filled with aCSF. For whole-cell current-clamp recordings, a K^+-based internal solution (in mM: 119 $KMeSO_4$, 5 KCl, 0.16 $CaCl_2$, 10 HEPES, 0.5 EGTA, 12 phosphocreatine (Na_2), 2 MgATP, 0.7 Na_2GTP, pH 7.3 adjusted with KOH, 290 mOsm) was used. For whole-cell voltage-clamp recordings, a Cs^+-based internal solution (in mM: 108 $CsMeSO_4$, 15 CsCl, 5 TEA-Cl, 20 HEPES, 0.4 EGTA, 2.5 MgATP, 0.25 Na_3GTP, 1 QX-314, 7.5 phosphacreatine (Na_2), 1 L-Glutathione; pH 7.25 – 7.30; 290 mOsm) was used. To examine the current-voltage relationship of mGluR5-coupled conductances, Cs^+-based internal solution was used, and the neuron was stabilized at 20 mV before ramping down to −100 mV in 5 sec. To test DREADDs (Gq) activation of MCH neurons, clozapine N-oxide (CNO) was bath applied at 10 μM. To test ChR2-activation of MCH neurons, TTL-controlled laser light of 473 nm (blue; Shanghai Laser & Optics) was delivered as 1 ms pulses through the 40x objective lens onto the slice. At least 1–5 min of a stable baseline was recorded for each data collection. In all recordings, series resistance was 8 – 15 MΩ and was left uncompensated. Series resistance was monitored continuously during all recordings, and a change beyond ±20% resulted in exclusion of the cell from data analysis. Synaptic currents were recorded with a MultiClamp 700B amplifier or an Axopatch 200B amplifier (Molecular Devices), filtered at 2.6 – 3 kHz, amplified at 5 ×, and then digitized at 20 kHz with a Digidata 1440A or Digidata 1332 analog-to-digital converter (Molecular Devices). Electrophysiological data were analyzed using Clampfit (9/10), and similar as previously described[40, 47–49].

All drugs were bath-applied. Picrotoxin (100 μM) was used to inhibit $GABA_A$ receptors, NBQX (5 μM) and D-APV (50 μM) were used to block AMPA receptors and NMDA receptors. Tetrodotoxin (TTX, 1 μM) was used to isolate the miniature events. CHPG (100 μM) and MPEP (10 μM) were mGluR5 agonist and antagonist respectively. CHPG was applied in the presence of AMPA, NMDA, and $GABA_A$ receptor antagonists to isolate the mGluR5-coupled current. NBQX, D-APV, CHPG, and MPEP were purchased from Tocris-Fisher Scientific. TTX was purchased from Alomone Labs. CNO was obtained from the Chemical Synthesis and Drug Supply Program of the National Institute of Mental Health as well as from Tocris-Fisher Scientific. All other reagents were purchased from Sigma-Aldrich.

Sleep recordings and analysis

Methods for sleep recordings and analysis are similar as previously described[6, 38–40]. Rats were allowed to habituate in the recording chamber (7”x15”x7”) for 3 days after being tethered before recording started. EEG and EMG signals were amplified using Grass model 15LT bipolar amplifiers (Grass Technologies, West Warwick, RI) and an analog-digital converter (Kissei Comtec). The EEG was filtered below 0.1 Hz and above 30 Hz. The EMG was filtered below 30 Hz and above 3 kHz. All signals were digitized at 128 Hz and collected using Vital Recorder software (Kissei Comtec, Nagano, Japan) or SleepMaster (Biosoft Studio, PA, USA). All signals were auto scored for sleep states in 10-sec epochs using Somnivore 2.0 (Somnivore Inc., Australia) and visually inspected by an experienced

investigator. Wakefulness was identified by desynchronized EEG and high EMG activity; NREM sleep exhibited high amplitude slow waves and lower EMG; REM sleep exhibited regular EEG theta activity and extremely low EMG activity. Consolidated NREM sleep and wake episodes were determined by the same state in a stretch of time of no less than 30 sec (3 epochs). For EEG power spectrum analysis, EEG signals underwent Fast Fourier Transformation (FFT) using 0.5 Hz frequency bins (0–63.5 Hz), and normalized to the baseline sleep 24-hr state average. NREM/REM sleep latency was measured as the time to the first 1-min NREM or REM episode. Overall sleep latency was measured as the time to the first 3-min sleep episode containing both NREM and REM. All rats were coded for sleep scoring, and then decoded for data compiling.

In vivo chemogenetics

CNO was obtained from the Chemical Synthesis and Drug Supply Program of the National Institute of Mental Health as well as from Tocris-Fisher Scientific. A working solution of 0.5 mg/ml (1.47 mM) of CNO in saline was prepared freshly before each experiment (injection dose: 1 mg/2 ml/kg body weight). Vehicle (saline) or CNO-containing saline was injected subcutaneously at 5 pm, 2 hrs before light onset.

In vivo optogenetics

The setup and parameters for in vivo optogenetics were similar as described previously[40, 43]. A 473 nm blue laser (Shanghai Laser & Optics), TTL-controlled by a pulse-generator (Master-8, A.M.P.I., or DG1022, Rigol), was coupled to a branching fiberoptic patchcord (Doric Lenses) through a fiber optic rotary joint (Prizmatix). Light intensity at the exit of each branch was adjusted to ~6 mW, which reached ~5 mW at the exit of the fiberoptic implants (~80% transmission). Bilateral fiberoptic implants delivered trains of light pulses (1 ms pulses at 10 Hz, 5 sec on 5 sec off) selectively during sleep. Closed-loop stimulation system was modified from a previously described system[9]. Real-time sleep scoring was performed using SleepMaster program (Biosoft Studio, Hershey, PA), and based on weighted considerations of EEG amplitude, EMG amplitude, delta power (0.5–4 Hz), theta power (4.5–8 Hz), beta power (30–50 Hz), and EEG variation (SD/Mean). Correct stim: ≥ 3 secs of stimulation in a 10-sec NREM or REM epoch; correct non-stim: ≤ 3 secs of stimulation within a 10-sec Wake epoch; false stim: > 3 secs of stimulation in Wake epochs; false non-stim: < 3 secs of stimulation during sleep epochs. For additional within-subject controls, rats received handling and patchcord attachment during baseline without getting laser stimulation.

Feeding test

Rats were singly housed with ad libitum access to lab chow and water. The amount of lab chow was weighed at ZT 22 (5 pm), immediately before CNO/saline injection or in vivo laser stimulation session, and then again at 4 hrs and 12 hrs after.

Data analysis and statistics

Rats were randomly assigned to all experimental groups. Group sizes were determined based on power analyses using preliminary estimates of variance with the goal of achieving 80%

power to observe differences at α=0.05. No data points were excluded unless specified in the experimental procedure. Out of 168 total rats that were used, 4 rats did not establish cocaine self-administration and were excluded from further experimentation, 4 rats yielded poor slice preparation or poor-quality electrophysiological recordings and were excluded before data collection, 25 rats were excluded from sleep data analysis because of losing the headpiece, poor EEG/EMG signals, or misplacement/damage of the implants, 4 rats were excluded from RNA-sequencing because of RIN numbers being lower than 7 or tissue damage. RNA-sequencing experiment was replicated in 4 rats, electrophysiological recordings in at least 6 rats, and sleep recordings in 4–8 rats. All data were analyzed blind to treatment groups. Statistical analysis was performed using Prism GraphPad (7/8). Normal distribution was assumed for all statistics based on visual inspection and previous experience, and was not formally tested[40, 50]. Homoscedasticity (equality of variance) was tested using Fisher's *F* test (between 2 groups) or Levene's test (3 or more groups) prior to *t* test or ANOVA test respectively (*F* and Levene's testing results not shown). Statistical significance was assessed using *t* tests (for two-group comparisons; two-tailed tests), one-way ANOVA (single factor multiple groups), or two-way ANOVAs with or without repeated measures (RM), followed by posttests based on individual recommendations by Prism. $p < 0.05$ was considered statistically significant. For electrophysiological recordings using behaviorally treated rats, animal-based statistics were reported, and both cell and animal numbers were reported. For recordings using slice-based treatment, slice-based analyses were reported. All others used animal-based analyses. Numbers of cells (n) and animals (m) are presented as "n/m". All data are shown as mean ± SEM.

Results

Cocaine experience persistently alters gene expression in LH MCH neurons.

To assess cocaine-induced gene expression changes in MCH neurons, we injected AAV5-MCHp-GFP into the LH and zona incerta regions (LH in brief) to selectively express GFP in LH MCH neurons. We observed that ~96% of GFP-labeled cells also showed MCH immunoreactivity, suggesting high specificity of GFP expression in LH MCH neurons (Fig. 1a–b). Following self-administration training and 3-week withdrawal, GFP-labeled neurons from saline- or cocaine-trained rats were laser-microdissected from thin sections for RNA-sequencing (Fig. 1c; Supplementary Fig. 1a). We chose this time point as the sleep patterns at 3-week withdrawal are stabilized and similar to that at longer-term withdrawal[6], and the age of the rats still allows for slice electrophysiological recordings from the myelin-rich LH regions to validate potential findings in gene expression changes and probe for functional alterations (see below). As expected, all samples showed high expression levels of *GFP* and the MCH precursor Pro-melanin concentrating hormone (*Pmch*), and other predicted transcripts including cocaine- and amphetamine-regulated transcript (*Cart*) etc.[26, 27, 51–56]. By contrast, samples showed low levels of genes expressed by other cell types in LH (Fig. 1d; [57–59]). These results suggest the specificity of the cell sampling.

Differential expression (DE) analysis showed 213 down-regulated and 241 up-regulated genes in LH MCH neurons following cocaine training and withdrawal compared to saline-treated rats (Fig. 1e). There was high confidence in the identified DE genes, as

the top 75 most robust DE genes showed natural segregations between cocaine and saline-treated rats examined by unsupervised clustering (Supplementary Fig. 2). Overall, the top differentially expressed genes spread to a variety of cell-signaling regulatory categories, including gene transcription regulations, post-translational modifications, Golgi secretion, G protein-coupled receptors and signaling, kinases, extracellular matrix, energy production, protein degradation, and DNA repair (Supplementary Tables 1,2). We then used the DAVID database to identify enriched functional gene ontology, and to determine if specific biological processes were the target of cocaine-induced alterations in LH MCH neurons. This analysis showed persistent impact of cocaine experience onto several essential regulatory pathways in these neurons, mediating potential changes in axon ensheathment, cell surface receptor signaling, transcriptional and post-translational regulations, and cell morphogenesis etc. (Fig. 1f–g).

Related to electrophysiological membrane properties and neurotransmissions, there were altered expressions of voltage-gated K^+ channels, voltage-gated Ca^{2+} channels, and ionotropic and metabotropic glutamate receptors, as well as some subtle changes in GABA receptors and metabotropic acetylcholine receptors. Expression of AMPA receptors, dopamine receptors, and other neurotransmitter receptors were largely not different between cocaine- and saline-treated rats after 3-week withdrawal (Fig. 1h). These results suggest that cocaine experience persistently alters gene expressions in LH MCH neurons, some of which may result in changes in the membrane excitability as well as glutamatergic transmission onto these neurons.

Cocaine experience persistently reduces membrane excitability and impairs glutamate receptor activity in LH MCH neurons.

We then used slice electrophysiology to assess cocaine-induced changes in LH MCH neuron functions. AAV5-MCHp-GFP was injected into the LH to selectively label MCH neurons with GFP. Acute brain slices were prepared following cocaine self-administration and 3 weeks of withdrawal (Fig. 2a; Supplementary Fig. 1b–d). The spontaneous firing patterns of LH MCH neurons in slices were diverse, exhibiting regular firing, burst, irregular firing, or no firing; and in cocaine-treated rats there was a shift toward less regular firing and more non-firing MCH neurons (Fig. 2b). Furthermore, whole-cell current-clamp recordings showed a decrease in the current-evoked action potential firing in cocaine-treated rats compared to saline-treated ones, suggesting reduced membrane excitability (cocaine x current interaction: $F_{20, 280}=5.057$, $p<0.001$; cocaine effect at 220–400 pA: $p<0.05$; two-way RM ANOVA with Sidak post-test; Fig. 2c,d). Similar reductions were not detected at 1 week after withdrawal (Supplementary Fig. 3), suggesting that it is a consequence of long-term withdrawal. The reduced excitability was associated with a more depolarized action potential threshold in the cocaine-treated group ($t_{14}=3.117$, $p<0.01$), and a higher rheobase current ($t_{14}=2.636$, $p<0.05$, unpaired *t* test; Fig. 2e), but otherwise similar action potential shapes and after-hyperpolarizations (Supplementary Table 3). The higher rheobase current and more depolarized action potential threshold (with no changes in Rm) is also consistent with increased expression of voltage-gated potassium channels such as *Kcna1*.

We then examined the excitatory and inhibitory synaptic transmissions onto the LH MCH neurons. There was no change in the miniature EPSCs amplitude or frequency (amplitude: t_{18}=0.226, p=0.824; frequency: t_{18}=0.148, p=0.884; unpaired *t* test; Fig. 2f), and no change in the miniature IPSC amplitude or frequency (amplitude: t_{11}=0.620, p=0.548; frequency: t_{11}=0.503, p=0.625; unpaired *t* test) (Fig. 2g), suggesting normal basal transmissions through synaptic AMPA receptors and $GABA_A$ receptors. Nonetheless, there was a reduction of synaptic NMDA receptor transmission relative to AMPA receptor transmission, evidenced by a decrease in the NMDA/AMPA ratio in evoked synaptic currents (t_{20}=3.568, p<0.01; unpaired *t* test; Fig. 2h). The decrease in synaptic NMDA receptor activity was in contrast to the gene expression results, where no decrease in NMDAR subunit expression was detected (*Grin3b* was increased, no change in other subunits). These results may suggest a deficit in the translation, trafficking, and/or positive modulation of NMDARs in cocaine-treated rats.

To examine mGluR5 activity in MCH neurons, we bath-applied mGluR5-selective agonist CHPG (100 μM) in the presence of AMPA, NMDA, and $GABA_A$ receptor antagonists, which induced a depolarizing current (reversal potential ~ −10 mV, not corrected for junctional potential) in GFP-labeled LH MCH neurons (Fig. 2i), presumably through mGluR5-coupled electrogenic transporters (Na^+/Ca^{2+} exchanger) in LH MCH neurons [60]. The current was expectedly sensitive to blockade by pre-application of MPEP (10 μM), a selective mGluR5 antagonist, (n=8 slices; Fig. 2j). The CHPG-induced mGluR5 current was reduced in the cocaine-treated rats after 3-week withdrawal compared to the saline ones (cocaine x current interaction: $F_{20, 240}$=5.756, p<0.001; cocaine effect at −75 mV to −100 mV: p<0.05; two-way RM ANOVA with Sidak post-test; Fig. 2k), suggesting cocaine-induced reduction of functional mGluR5 receptors on MCH neurons.

Together, these results suggest that cocaine experience persistently reduces LH MCH neuron membrane excitability and impairs glutamatergic signaling through mGluR5 receptors and synaptic NMDARs.

Chemogenetic activation of LH MCH neurons during the light (inactive) phase promotes both wakefulness and REM sleep after long-term cocaine withdrawal.

The above transcriptional and functional analyses suggest that LH MCH neurons undergo persistent functional impairment after withdrawal, including weakened excitatory inputs, dampened membrane excitability, and altered axon myelination processes. Thus, are these neurons still capable of positively regulating REM sleep after long-term withdrawal? To test this, we injected AAV5-MCHp-DREADDs(Gq)-mCherry into the LH to selectively express DREADDs (Gq) in MCH neurons. The specificity of DREADDs (Gq) expression was confirmed by the majority (~90%) of mCherry-labeled cells also showing MCH immunoreactivity (Fig. 3a–b). In acute LH slices, bath application of the DREADDs selective ligand CNO (10 μM) facilitated spontaneous action potential firing in mCherry-labeled cells (t_7=5.417, p<0.01, paired *t* test; Fig. 3c–d), presumably through Gq-mediated membrane depolarization (t_{14}=2.275, p<0.05, unpaired *t* test; Fig. 3e; [61]).

We then tested the effect of chemogenetic activation of MCH neurons on sleep *in vivo* after long-term withdrawal of ~45 days, when withdrawal-associated long-term behavioral

changes (e.g. cue-induced drug seeking) become prominent [6, 62]. After cocaine self-administration training and 45 days of withdrawal (Supplementary Fig. 1e), rats received saline or CNO (1 mg/kg) injections on two consecutive days soon before light onset at ~ zeitgeber time (ZT) 22 (Fig. 3f), and 24-hr sleep after each injection was compared upon normalization to the baseline sleep 24 hrs before the first injection. As expected, the total amount of 24-hr REM sleep time was increased following CNO injection compared to saline (t_5=6.258, p<0.01; paired t test), mostly during the dark phase (light: t_5=1.965, p=0.107; dark: t_5=7.091, p<0.001; paired t tests; Fig. 3g). Total NREM sleep was reduced (t_5=7.475, p<0.001; paired t test), predominantly due to the loss of NREM sleep during the light phase (light: t_5=11.170, p<0.001; dark: t_5=4.082, p<0.01; paired t tests; Fig. 3h). There was an increase in total wakefulness (t_5=4.334, p<0.01; paired t test), due to large increase of wake time in the light phase (light: t_5=10.345, p<0.001; dark: t_5=7.071, p<0.001; paired t tests; Fig. 3i). Bout analysis (Fig. 3j,k) revealed that both the total number and average bout duration of REM episodes were increased following CNO injection (number: t_5=3.678, p<0.05; duration: t_5=2.972, p<0.05; paired t tests), whereas NREM sleep showed no change in the number of episodes but a decrease in the average episode duration (number: t_5=0.549, p=0.607; duration: t_5=4.474, p<0.01; paired t tests). Wake bout number and duration did not differ between saline and CNO injections (number: t_5=1.825, p=0.128; duration: t_5=0.707, p=0.511; paired t tests). Finally, 24-hr state power spectrum analysis (Fig. 3l–n) revealed slightly shifted theta range power distribution during REM sleep (interaction $F_{99, 500}$=3.249, p<0.001; p<0.001~0.05 at 0.5, 1.5, 6, and 7–7.5 Hz), and increased delta power during NREM sleep (interaction $F_{99, 500}$=4.930, p<0.001; p<0.001~0.05 at 0.5–5 Hz), presumably serving to compensate for the decrease in NREM sleep time. Additionally, there was an increase of power in the delta and theta range during wakefulness following CNO administration (interaction $F_{99, 500}$=11.393, p<0.001; p<0.001~0.05 at 2.5–4.5 and 6–9.5 Hz; two-way RM ANOVA with Sidak post-test). By contrast, the changes in wakefulness were not observed in rats lacking MCHp-DREADDs expression (Supplementary Fig. 4), nor in rats receiving MCH stimulation selectively during sleep (see below), suggesting that it results from DREADDs activation of MCH neurons during wakefulness.

To better understand CNO's dual effects on wakefulness and REM sleep, we examined the sleep time in 2-hr bins across 24 hrs post-injection (Fig. 3o–q). Although CNO was injected soon before light onset, it induced a potent pro-wakefulness effect (overall sleep latency: t_5=10.012, p<0.001; paired t test) that lasted for ~5 hrs (Fig. 3q), and delayed both NREM and REM sleep onsets (NREM latency: t_5=10.021, p<0.001; REM latency: t_5=6.739, p<0.01; paired t tests; Fig. 3o,p). This was followed by a dramatic increase in REM and a moderate increase in NREM sleep time through the rest of light and dark phases (wake: CNO x time interaction: $F_{11, 55}$ = 39.531, p < 0.001; NREM: CNO x time interaction: $F_{11, 55}$ = 43.287, p < 0.001; REM: CNO x time interaction: $F_{11, 55}$ = 8.740, p < 0.001; two-way RM ANOVA with Sidak post-tests; Fig. 3o–q). The pro-wakefulness effect of CNO was likely through activation of DREADDs (Gq), as rats that did not express DREADDs (Gq) did not show this effect (Supplementary Fig. 4). The wake-promoting effect was also not separable from the REM sleep-promoting effect by varying doses of CNO, and the CNO effects appeared to be most apparent during the light phase (Supplementary Fig. 5–6). Thus,

Gq-activation of LH MCH neurons has dual effects: it promotes both wakefulness and REM sleep.

MCH neural activity as well as MCH peptide signaling have been shown to promote feeding[63–65]. Could the pro-wakefulness effect of MCH neural activation be associated with enhanced feeding activity? To test this, we measured the amount of food consumption after CNO or saline injections. Indeed, CNO-treated rats showed more cumulative food pellet consumption compared to saline-treated rats measured at 4 hrs post injection, followed by reduced food intake in the next 8 hrs (4 hr: $F_{3, 26}$=6.515, p<0.01; next 8 hr: $F_{3, 26}$=4.009, p<0.05; one-way RM ANOVA with Sidak post-tests; Fig. 3r). Thus, to selectively enhance REM sleep without promoting wakefulness and feeding, it may be necessary to selectively stimulate LH MCH neurons during sleep.

Optogenetic activation of LH MCH neurons during sleep selectively increases REM sleep after long-term cocaine withdrawal.

The above results suggest that enhancing LH MCH neural activity has dual effects on behaviors, which is potentially vigilance state-dependent. To focus on the REM sleep-enhancing effect, we then attempted to stimulate LH MCH neural activity selectively during sleep, which was better achieved using optogenetic approach. We injected AAV5-MCHp-ChR2-EYFP into the LH bilaterally. The specificity of ChR2 expression was confirmed by the majority of EYFP-labeled cells also showing MCH immunoreactivity (Fig. 4a–b). In acute LH slices, 473 nm laser stimulation at 10 and 20 Hz elicited high-fidelity action potential firing in EYFP-labeled neurons (1 ms x 10 or 20 Hz, 5 s-ON-5 s-OFF, for 2–5 min, i.e. typical REM and NREM episode durations; Fig. 4c). To stimulate selectively during sleep, we used a closed-loop stimulation system driven by the rat EEG/EMG signals and processed by a real-time auto-scoring computer algorithm (see Methods; Fig. 4d). Manual inspection of sleep states post-recordings confirmed that the real-time, auto-scored sleep states achieved high accuracy (>90% of total # epochs for each individual rat across 12 hrs), and triggered laser outputs accordingly in both naïve and cocaine-treated rats (Fig. 4e–f; Supplementary Fig. 7b,d).

We then tested the effect of optogenetic activation of MCH neurons on sleep *in vivo*. In naïve rats expressing MCHp-ChR2, bilateral laser stimulation (10 Hz, 5 sec on, 5 sec off) of LH MCH neurons selectively during sleep increased REM sleep without affecting food or water intake (Supplementary Fig. 7). In rats after long-term withdrawal from cocaine self-administration (Supplementary Fig. 1f), we used the same protocol to stimulate LH MCH neurons selectively in sleep during the 12-hr light phase (Fig. 5a). The 24-hr sleep time after onset of first laser stimulation (~ ZT 0) was compared to the 24-hr baseline sleep before laser stimulation. Sleep-stimulation of LH MCH neurons in the light phase increased total 24-hr REM sleep time (t_7=6.053, p<0.001; paired t test) by increasing light-phase REM sleep (light: t_7=5.160, p<0.01; dark: t_7=0.262, p=0.801; paired t tests; Fig. 5b). This is at the cost of a small amount of NREM sleep in the light phase, which was compensated by dark-phase NREM sleep rebound (light: t_7=4.078, p<0.01; dark: t_7=5.348, p<0.01; paired t tests), leading to no change in total 24-hr NREM sleep (t_7=0.225, p=0.828, paired t test; Fig. 5c). There was also a decrease in 24-hr total wakefulness (t_7=4.209, p<0.01;

paired *t* test), mostly driven by decreased dark-phase wakefulness due to NREM rebound presumably (light: t_7=0.510, p=0.626; dark: t_7=5.525, p<0.001; paired *t* tests; Fig. 5d). Together, there was increase in total REM sleep at a small cost of wakefulness time. Bout analysis for the 12-hr light phase (Fig. 5e–f) revealed that the increase in REM sleep was through increased REM bout number as well as lengthened average bout duration (number: t_7=3.330, p<0.05; duration: t_7=3.080, p<0.05; paired *t* tests), which was at the cost of light-phase NREM sleep (bout number: t_7=2.704, p<0.05; bout duration: t_7=3.906, p<0.01; paired *t* tests). Sustained wakefulness showed decreased number of episodes, though no change in average bout durations (number: t_7=3.170, p<0.05; duration: t_7=1.215, p=0.264; paired *t* tests). 24-hr bout analysis (Fig. 5g–h) showed similar changes, except that the increase in REM episode duration was not apparent when averaged over 24 hrs (t_7=0.438, p=0.675; paired *t* tests). Power spectrum analysis (Fig. 5i–k) over 24 hrs showed that laser stimulation increased higher-frequency theta power during REM sleep (interaction $F_{99, 700}$=5.097, p<0.001; p<0.001~0.05 at 6–6.5, 7.5–9, 9.5–10, and 11 Hz), increased low wave power subtly during NREM sleep (interaction $F_{99, 700}$=1.708, p<0.001; p<0.001 at 0–1.5 Hz; two-way RM ANOVA with Sidak post-tests), and did not change the power spectrum in wakefulness (interaction $F_{99, 700}$=0.965, p=0.578). Finally, in contrast to the CNO effect, sleep-stimulation of LH MCH neurons maintained the overall sleep onset (t_7=1.437, p=0.194; paired *t* test), promoted REM sleep onset (t_7=6.877, p<0.001; paired *t* test) without affecting NREM sleep onset (t_7 = 0.248, p = 0.811; paired t test). It effectively increased REM sleep throughout the 12-hr light phase, and did not induce negative rebound during the following dark phase (laser stim x time interaction: $F_{11, 77}$=6.860, p<0.001; p<0.001~0.05 at hr 1–11; two-way RM ANOVA with Sidak post-test; Fig. 5l–n). Laser stimulation in cocaine-trained rats without MCHp-ChR2 expression had no effect on sleep (Supplementary Figs. 1g, 8).

Thus, optogenetic activation of LH MCH neurons selectively during sleep increases REM episode numbers, durations, and theta power, which together, increases, consolidates, and enhances REM sleep in rats after long-term withdrawal from cocaine.

Discussion

The persistent sleep abnormalities that manifest after withdrawal from chronic drug use may present new opportunities for drug addiction treatment development[66, 67]. Here we characterize changes in gene expression profiles and electrophysiological properties in LH MCH neurons that predict hypoactivity of these neurons after long-term withdrawal from cocaine, and specify an *in vivo* approach that effectively promotes REM sleep with minimal side-effects after cocaine withdrawal.

Cocaine-induced persistent changes in LH MCH neurons

MCH neurons express a variety of receptors that allow them to sense and respond to a wide range of neural chemical level changes sampled throughout the brain[20, 27, 28]. It is, therefore, not surprising that LH MCH neurons are impacted by cocaine experience and withdrawal.

Three weeks after withdrawal from cocaine, LH MCH neurons exhibit dampened spontaneous firing in slices, likely resulting from reduced membrane excitability and more

depolarized action potential threshold (Fig. 2). Gene analysis reveals increased expression of the voltage-gated K^+ channel *Kcna1* after cocaine withdrawal (Fig. 1e, h), consistent with the reduced membrane excitability. Furthermore, LH MCH neurons exhibit deficient glutamatergic signaling through mGluR5 and synaptic NMDA receptors (Fig. 2), whereas gene analysis reveals down-regulation of *Grm5* but not genes encoding NMDA receptor subunits. It is not known whether reduced synaptic NMDAR transmission may be related to a potential reduction of mGluR5-NMDA receptor interaction that has been shown to potentiate NMDA receptor function in LH MCH neurons and elsewhere[60, 68].

Beyond glutamatergic transmission and membrane excitability, a broad range of cellular processes are presumably altered in LH MCH neurons after withdrawal from cocaine, including DNA repair, transcription regulation, cell energy metabolism, transmembrane signaling, kinase signaling, and cellular secretion etc. (Fig. 1f–g). One prominent set of changes is the up-regulation of many genes in the myelin-regulatory pathway. It is noteworthy that several of the up-regulated myelin-regulatory genes are predominantly enriched in oligodendrocytes. It is possible that we have unintendedly included some surrounding oligodendrocytes (from both saline and cocaine-treated rats) during laser microdissection of LH MCH neurons. While oligodendrocytes were not the dominant populations within our samples, there were, nonetheless, sufficient counts to reveal significant changes in myelin-regulatory gene expression following cocaine withdrawal.

Chronic cocaine use often leads to changes indicative of impairment in white matter integrity and myelin-related gene expression in various brain regions in humans and animals[69–73]. Interestingly, we observed up-regulation of many myelin pathway genes (Supplementary Tables 1,2). It is not clear whether these changes may represent functional compensations after long-term cocaine withdrawal. Indeed, up-regulation of myelin-associated protein expressions have also been observed after protracted abstinence from chronic alcohol use[74]. It remains to be determined whether LH MCH neurons may have altered action potential conducting properties resulting from myelin changes after withdrawal from cocaine, and whether similar changes occur in LH neuronal populations other than MCH neurons.

MCH neurons are located in similar LH regions as hypocretin/orexin neurons, and the two groups of neurons form reciprocal connections and often functionally oppose each other (reviewed in[75]). While hypocretin/orexin neurons promote arousal and reward seeking, MCH neurons inhibit hypocretin/orexin neurons, promote sleep, induce depressive-like behaviors, though facilitate food reward[63, 76–78]. LH hypocretin/orexin neurons exhibit increased number and enhanced activity in rats following cocaine self-administration and withdrawal[79]. Complementarily, we observed reduced membrane excitability and impaired glutamatergic signaling in MCH neurons (Figs. 1,2), suggesting hypofunction of MCH neurons after withdrawal. Thus, changes in LH hypocretin/orexin neurons and MCH neurons may synergistically contribute to altered sleep and reward processing after long-term withdrawal from cocaine.

Enhancing LH MCH neural activity to promote REM sleep after long-term withdrawal from cocaine

May reduced MCH neural activity contribute to impaired REM sleep after long-term cocaine withdrawal? In drug-naive animals, suppressing MCH neural activity or eliminating these neurons altogether does not change REM sleep[34]. Thus, it is possible that hypoactivity of LH MCH neurons is not the leading cause for impaired REM sleep after cocaine withdrawal. Nonetheless, rats after cocaine exposure experience long-lasting overall sleep changes[6], possibly involving multiple sleep regulatory mechanisms. LH MCH neurons are known to respond to and regulate REM sleep deprivation-induced rebound[35–37]. Thus, it is possible that impaired MCH neural activity may contribute to the chronic nature of REM sleep disturbance, with presumed impairment in the homeostatic REM sleep control.

We found that increasing LH MCH neural activity by either chemogenetic or optogenetic approaches increases REM sleep. However, the chemogenetic approach also induces a pro-wakefulness effect and delays overall sleep and REM sleep onsets (Fig. 3). By contrast, optogenetic stimulation of LH MCH neurons selectively during sleep shortens REM sleep onset, increases total REM sleep time, REM sleep bouts, and REM bout durations, without promoting feeding or prolonged wakefulness (Fig. 5; Supplementary Fig. 7), and thus is the preferred way for improving REM sleep after withdrawal. Comparing the differential effects by optogenetic vs. chemogenetic approaches, potential contributing factors may include 1) differences in the stimulation subregions, i.e. zona incerta vs. extended LH regions, which may differentially engage diverse populations of MCH neurons[56, 58], and have differential behavioral impacts; 2) differences in the evoked firing patterns (10 Hz, 5 sec on/off vs. tonic activation) – neural peptides release is often facilitated by high frequency bursts compared to tonic low frequency firing[80–82]. It is therefore possible that optogenetically induced high frequency bursts of MCH neurons may result in higher MCH release compared to chemogenetic stimulations, and MCH co-release may further facilitate REM sleep[25, 83]; 3) it is possible that stimulating MCH neural activity may produce distinct behavioral outcomes depending on the vigilance state of the animal and/or circadian phases, such that stimulating MCH activity during sleep would enhance REM sleep, whereas stimulating during wakefulness may preferentially increase feeding and other behaviors. These potential scenarios may help us better appreciate the diverse roles of the MCH system in regulating sleep, mood, and reward processing.

What may be the reason(s) for CNO-induced delayed REM sleep increase? Could it be because of diminished CNO effect over time (i.e. receptor desensitization and CNO wash off)? Or perhaps the REM sleep increase is entirely driven by REM sleep rebound following the initial deprivation (Fig. 3o)? First, it is not likely that a tampered CNO effect may be driving the REM sleep rebound, as lower doses of CNO alone were less effective to drive REM sleep increase (Supplementary Figs. 5–6). Moreover, in the absence of CNO-stimulation, we observed that REM sleep restriction alone (to ~40% of baseline REM sleep for 12 hr) in cocaine-withdrawn rats induces REM sleep rebound, and yet the 24-hr total REM sleep is not changed[6], which is in contrast to the CNO-induced increase in 24-hr total REM sleep (Fig. 3g). Thus, it is most likely that the residual CNO effect (> 6 hr) combined with increased sleep debt may together drive REM sleep potentiation.

MCH neural activity during REM sleep may impact behaviors during subsequent wakefulness. For example, REM-active LH MCH neurons are shown to weaken contextual memory[84]. We also reported previously that REM sleep changes induced by sleep restriction/rebound result in altered cocaine craving after withdrawal[6]. Thus, current results demonstrate that LH MCH stimulation may help alleviate cocaine-induced REM sleep impairment after withdrawal, which may be explored for potential benefits for regulating relapse-like behaviors.

Supplementary Material

Refer to Web version on PubMed Central for supplementary material.

Acknowledgement:

We thank Dr. Priyattam J. Shiromani for kindly providing us with the AAV5-MCHp-GFP and AAV5-MCHp-ChR2-EYFP constructs; Dr. Oliver M. Schlüter for advice on molecular cloning; Dr. Ryan W. Logan for helpful discussions on transcriptome analysis; Dr. John F. Enwright, Dominique Arion for technical guidance on laser microdissection; Wei Zong for transcriptome analysis technical support; Braden R Bubarth, Rachel L Hines, and Jake Minnick for help with rat behavioral trainings; Dr. Zheng Liu for technical support with slice electrophysiology. Research reported in this publication was supported by the National Institutes of Health under Award Numbers DA043826 (YH), DA046491 (YH), AA028145 (YH), MH120066 (MLS), LM012752 (GCT), DA023206 (YD), DA040620 (YD), DA047861 (YD). Cocaine was supplied by the Drug Supply Program of NIH NIDA. Clozapine N-oxide was partly supplied by the Chemical Synthesis and Drug Supply Program of NIMH.

References

1. Angarita GA, Emadi N, Hodges S, Morgan PT. Sleep abnormalities associated with alcohol, cannabis, cocaine, and opiate use: a comprehensive review. Addict Sci Clin Pract 2016; 11(1): 9. [PubMed: 27117064]
2. Jaehne A, Unbehaun T, Feige B, Cohrs S, Rodenbeck A, Schutz AL et al. Sleep changes in smokers before, during and 3 months after nicotine withdrawal. Addict Biol 2015; 20(4): 747–755. [PubMed: 24797355]
3. Angarita GA, Canavan SV, Forselius E, Bessette A, Pittman B, Morgan PT. Abstinence-related changes in sleep during treatment for cocaine dependence. Drug and alcohol dependence 2014; 134: 343–347. [PubMed: 24315572]
4. Kowatch RA, Schnoll SS, Knisely JS, Green D, Elswick RK. Electroencephalographic sleep and mood during cocaine withdrawal. Journal of addictive diseases 1992; 11(4): 21–45. [PubMed: 1486092]
5. Matuskey D, Pittman B, Forselius E, Malison RT, Morgan PT. A multistudy analysis of the effects of early cocaine abstinence on sleep. Drug and alcohol dependence 2011; 115(1–2): 62–66. [PubMed: 21144676]
6. Chen B, Wang Y, Liu X, Liu Z, Dong Y, Huang YH. Sleep Regulates Incubation of Cocaine Craving. The Journal of neuroscience : the official journal of the Society for Neuroscience 2015; 35(39): 13300–13310. [PubMed: 26424879]
7. Logan RW, Hasler BP, Forbes EE, Franzen PL, Torregrossa MM, Huang YH et al. Impact of Sleep and Circadian Rhythms on Addiction Vulnerability in Adolescents. Biological psychiatry 2018; 83(12): 987–996. [PubMed: 29373120]
8. Malcolm R, Myrick LH, Veatch LM, Boyle E, Randall PK. Self-reported sleep, sleepiness, and repeated alcohol withdrawals: a randomized, double blind, controlled comparison of lorazepam vs gabapentin. J Clin Sleep Med 2007; 3(1): 24–32. [PubMed: 17557449]
9. Puhl MD, Boisvert M, Guan Z, Fang J, Grigson PS. A novel model of chronic sleep restriction reveals an increase in the perceived incentive reward value of cocaine in high drug-taking rats. Pharmacology, biochemistry, and behavior 2013; 109: 8–15.

10. Puhl MD, Fang J, Grigson PS. Acute sleep deprivation increases the rate and efficiency of cocaine self-administration, but not the perceived value of cocaine reward in rats. Pharmacology, biochemistry, and behavior 2009; 94(2): 262–270.
11. Roehrs T, Johanson CE, Meixner R, Turner L, Roth T. Reinforcing and subjective effects of methylphenidate: dose and time in bed. Exp Clin Psychopharmacol 2004; 12(3): 180–189. [PubMed: 15301635]
12. Teplin D, Raz B, Daiter J, Varenbut M, Tyrrell M. Screening for substance use patterns among patients referred for a variety of sleep complaints. The American journal of drug and alcohol abuse 2006; 32(1): 111–120. [PubMed: 16450646]
13. Abel T, Havekes R, Saletin JM, Walker MP. Sleep, plasticity and memory from molecules to whole-brain networks. Current biology : CB 2013; 23(17): R774–788. [PubMed: 24028961]
14. Baran B, Pace-Schott EF, Ericson C, Spencer RM. Processing of emotional reactivity and emotional memory over sleep. The Journal of neuroscience : the official journal of the Society for Neuroscience 2012; 32(3): 1035–1042. [PubMed: 22262901]
15. Gujar N, McDonald SA, Nishida M, Walker MP. A role for REM sleep in recalibrating the sensitivity of the human brain to specific emotions. Cerebral cortex 2011; 21(1): 115–123. [PubMed: 20421251]
16. Siegel JM. Clues to the functions of mammalian sleep. Nature 2005; 437(7063): 1264–1271. [PubMed: 16251951]
17. Siegel JM. REM sleep: a biological and psychological paradox. Sleep medicine reviews 2011; 15(3): 139–142. [PubMed: 21482156]
18. Vyazovskiy VV, Delogu A. NREM and REM Sleep: Complementary Roles in Recovery after Wakefulness. The Neuroscientist : a review journal bringing neurobiology, neurology and psychiatry 2014; 20(3): 203–219.
19. Broberger C, De Lecea L, Sutcliffe JG, Hokfelt T. Hypocretin/orexin- and melanin-concentrating hormone-expressing cells form distinct populations in the rodent lateral hypothalamus: relationship to the neuropeptide Y and agouti gene-related protein systems. The Journal of comparative neurology 1998; 402(4): 460–474. [PubMed: 9862321]
20. Gonzalez JA, Iordanidou P, Strom M, Adamantidis A, Burdakov D. Awake dynamics and brain-wide direct inputs of hypothalamic MCH and orexin networks. Nat Commun 2016; 7: 11395. [PubMed: 27102565]
21. Haemmerle CA, Campos AM, Bittencourt JC. Melanin-concentrating hormone inputs to the nucleus accumbens originate from distinct hypothalamic sources and are apposed to GABAergic and cholinergic cells in the Long-Evans rat brain. Neuroscience 2015; 289: 392–405. [PubMed: 25613687]
22. Jego S, Glasgow SD, Herrera CG, Ekstrand M, Reed SJ, Boyce R et al. Optogenetic identification of a rapid eye movement sleep modulatory circuit in the hypothalamus. Nat Neurosci 2013; 16(11): 1637–1643. [PubMed: 24056699]
23. Bittencourt JC, Presse F, Arias C, Peto C, Vaughan J, Nahon JL et al. The melanin-concentrating hormone system of the rat brain: an immuno- and hybridization histochemical characterization. The Journal of comparative neurology 1992; 319(2): 218–245. [PubMed: 1522246]
24. Lagos P, Torterolo P, Jantos H, Monti JM. Immunoneutralization of melanin-concentrating hormone (MCH) in the dorsal raphe nucleus: effects on sleep and wakefulness. Brain research 2011; 1369: 112–118. [PubMed: 21078307]
25. Torterolo P, Scorza C, Lagos P, Urbanavicius J, Benedetto L, Pascovich C et al. Melanin-Concentrating Hormone (MCH): Role in REM Sleep and Depression. Front Neurosci 2015; 9: 475. [PubMed: 26733789]
26. Elias CF, Lee CE, Kelly JF, Ahima RS, Kuhar M, Saper CB et al. Characterization of CART neurons in the rat and human hypothalamus. The Journal of comparative neurology 2001; 432(1): 1–19. [PubMed: 11241374]
27. Harthoorn LF, Sane A, Nethe M, Van Heerikhuize JJ. Multi-transcriptional profiling of melanin-concentrating hormone and orexin-containing neurons. Cell Mol Neurobiol 2005; 25(8): 1209–1223. [PubMed: 16388333]

28. Guyon A, Conductier G, Rovere C, Enfissi A, Nahon JL. Melanin-concentrating hormone producing neurons: Activities and modulations. Peptides 2009; 30(11): 2031–2039. [PubMed: 19524001]
29. Kong D, Vong L, Parton LE, Ye C, Tong Q, Hu X et al. Glucose stimulation of hypothalamic MCH neurons involves K(ATP) channels, is modulated by UCP2, and regulates peripheral glucose homeostasis. Cell metabolism 2010; 12(5): 545–552. [PubMed: 21035764]
30. Hassani OK, Lee MG, Jones BE. Melanin-concentrating hormone neurons discharge in a reciprocal manner to orexin neurons across the sleep-wake cycle. Proceedings of the National Academy of Sciences of the United States of America 2009; 106(7): 2418–2422. [PubMed: 19188611]
31. Blanco-Centurion C, Luo S, Spergel DJ, Vidal-Ortiz A, Oprisan SA, Van den Pol AN et al. Dynamic Network Activation of Hypothalamic MCH Neurons in REM Sleep and Exploratory Behavior. The Journal of neuroscience : the official journal of the Society for Neuroscience 2019; 39(25): 4986–4998. [PubMed: 31036764]
32. Fraigne JJ, Peever JH. Melanin-concentrating hormone neurons promote and stabilize sleep. Sleep 2013; 36(12): 1767–1768. [PubMed: 24293745]
33. Konadhode RR, Pelluru D, Blanco-Centurion C, Zayachkivsky A, Liu M, Uhde T et al. Optogenetic stimulation of MCH neurons increases sleep. The Journal of neuroscience : the official journal of the Society for Neuroscience 2013; 33(25): 10257–10263. [PubMed: 23785141]
34. Tsunematsu T, Ueno T, Tabuchi S, Inutsuka A, Tanaka KF, Hasuwa H et al. Optogenetic manipulation of activity and temporally controlled cell-specific ablation reveal a role for MCH neurons in sleep/wake regulation. The Journal of neuroscience : the official journal of the Society for Neuroscience 2014; 34(20): 6896–6909. [PubMed: 24828644]
35. Kitka T, Adori C, Katai Z, Vas S, Molnar E, Papp RS et al. Association between the activation of MCH and orexin immunorective neurons and REM sleep architecture during REM rebound after a three day long REM deprivation. Neurochem Int 2011; 59(5): 686–694. [PubMed: 21740944]
36. Modirrousta M, Mainville L, Jones BE. Orexin and MCH neurons express c-Fos differently after sleep deprivation vs. recovery and bear different adrenergic receptors. The European journal of neuroscience 2005; 21(10): 2807–2816. [PubMed: 15926928]
37. Verret L, Goutagny R, Fort P, Cagnon L, Salvert D, Leger L et al. A role of melanin-concentrating hormone producing neurons in the central regulation of paradoxical sleep. BMC neuroscience 2003; 4: 19. [PubMed: 12964948]
38. Krueger JM, Obal F. A neuronal group theory of sleep function. Journal of sleep research 1993; 2(2): 63–69. [PubMed: 10607073]
39. Winters BD, Huang YH, Dong Y, Krueger JM. Sleep loss alters synaptic and intrinsic neuronal properties in mouse prefrontal cortex. Brain Res 2011; 1420: 1–7. [PubMed: 21962531]
40. Liu Z, Wang Y, Cai L, Li Y, Chen B, Dong Y et al. Prefrontal Cortex to Accumbens Projections in Sleep Regulation of Reward. The Journal of neuroscience : the official journal of the Society for Neuroscience 2016; 36(30): 7897–7910. [PubMed: 27466335]
41. Lee BR, Ma YY, Huang YH, Wang X, Otaka M, Ishikawa M et al. Maturation of silent synapses in amygdala-accumbens projection contributes to incubation of cocaine craving. Nat Neurosci 2013; 16(11): 1644–1651. [PubMed: 24077564]
42. Ma YY, Lee BR, Wang X, Guo C, Liu L, Cui R et al. Bidirectional Modulation of Incubation of Cocaine Craving by Silent Synapse-Based Remodeling of Prefrontal Cortex to Accumbens Projections. Neuron 2014.
43. Wang Y, Liu Z, Cai L, Guo R, Dong Y, Huang YH. A Critical Role of Basolateral Amygdala-to-Nucleus Accumbens Projection in Sleep Regulation of Reward Seeking. Biological psychiatry 2019.
44. Garrido-Gil P, Fernandez-Rodriguez P, Rodriguez-Pallares J, Labandeira-Garcia JL. Laser capture microdissection protocol for gene expression analysis in the brain. Histochem Cell Biol 2017; 148(3): 299–311. [PubMed: 28560490]
45. Lin LC, Sibille E. Somatostatin, neuronal vulnerability and behavioral emotionality. Mol Psychiatry 2015; 20(3): 377–387. [PubMed: 25600109]
46. Love MI, Huber W, Anders S. Moderated estimation of fold change and dispersion for RNA-seq data with DESeq2. Genome Biol 2014; 15(12): 550. [PubMed: 25516281]

47. Huang YH, Lin Y, Mu P, Lee BR, Brown TE, Wayman G et al. In vivo cocaine experience generates silent synapses. Neuron 2009; 63(1): 40–47. [PubMed: 19607791]
48. Huang YH, Ishikawa M, Lee BR, Nakanishi N, Schluter OM, Dong Y. Searching for presynaptic NMDA receptors in the nucleus accumbens. J Neurosci 2011; 31(50): 18453–18463. [PubMed: 22171047]
49. Suska A, Lee BR, Huang YH, Dong Y, Schluter OM. Selective presynaptic enhancement of the prefrontal cortex to nucleus accumbens pathway by cocaine. Proc Natl Acad Sci U S A 2013; 110(2): 713–718. [PubMed: 23267100]
50. Ghasemi A, Zahediasl S. Normality tests for statistical analysis: a guide for non-statisticians. Int J Endocrinol Metab 2012; 10(2): 486–489. [PubMed: 23843808]
51. Cvetkovic V, Brischoux F, Jacquemard C, Fellmann D, Griffond B, Risold PY. Characterization of subpopulations of neurons producing melanin-concentrating hormone in the rat ventral diencephalon. J Neurochem 2004; 91(4): 911–919. [PubMed: 15525345]
52. Croizier S, Franchi-Bernard G, Colard C, Poncet F, La Roche A, Risold PY. A comparative analysis shows morphofunctional differences between the rat and mouse melanin-concentrating hormone systems. PloS one 2010; 5(11): e15471. [PubMed: 21103352]
53. Broberger C Hypothalamic cocaine- and amphetamine-regulated transcript (CART) neurons: histochemical relationship to thyrotropin-releasing hormone, melanin-concentrating hormone, orexin/hypocretin and neuropeptide Y. Brain research 1999; 848(1–2): 101–113. [PubMed: 10612702]
54. Del Cid-Pellitero E, Jones BE. Immunohistochemical evidence for synaptic release of GABA from melanin-concentrating hormone containing varicosities in the locus coeruleus. Neuroscience 2012; 223: 269–276. [PubMed: 22890079]
55. Meister B Neurotransmitters in key neurons of the hypothalamus that regulate feeding behavior and body weight. Physiol Behav 2007; 92(1–2): 263–271. [PubMed: 17586536]
56. Mickelsen LE, Kolling FWt, Chimileski BR, Fujita A, Norris C, Chen K et al. Neurochemical Heterogeneity Among Lateral Hypothalamic Hypocretin/Orexin and Melanin-Concentrating Hormone Neurons Identified Through Single-Cell Gene Expression Analysis. eNeuro 2017; 4(5).
57. Marston OJ, Hurst P, Evans ML, Burdakov DI, Heisler LK. Neuropeptide Y cells represent a distinct glucose-sensing population in the lateral hypothalamus. Endocrinology 2011; 152(11): 4046–4052. [PubMed: 21914773]
58. Bonnavion P, Mickelsen LE, Fujita A, de Lecea L, Jackson AC. Hubs and spokes of the lateral hypothalamus: cell types, circuits and behaviour. The Journal of physiology 2016; 594(22): 6443–6462. [PubMed: 27302606]
59. Fakhoury M, Salman I, Najjar W, Merhej G, Lawand N. The Lateral Hypothalamus: An Uncharted Territory for Processing Peripheral Neurogenic Inflammation. Front Neurosci 2020; 14: 101. [PubMed: 32116534]
60. Huang H, van den Pol AN. Rapid direct excitation and long-lasting enhancement of NMDA response by group I metabotropic glutamate receptor activation of hypothalamic melanin-concentrating hormone neurons. The Journal of neuroscience : the official journal of the Society for Neuroscience 2007; 27(43): 11560–11572. [PubMed: 17959799]
61. Roth BL. DREADDs for Neuroscientists. Neuron 2016; 89(4): 683–694. [PubMed: 26889809]
62. Grimm JW, Hope BT, Wise RA, Shaham Y. Neuroadaptation. Incubation of cocaine craving after withdrawal. Nature 2001; 412(6843): 141–142. [PubMed: 11449260]
63. Barson JR, Morganstern I, Leibowitz SF. Complementary roles of orexin and melanin-concentrating hormone in feeding behavior. Int J Endocrinol 2013; 2013: 983964. [PubMed: 23935621]
64. Dilsiz P, Aklan I, Sayar Atasoy N, Yavuz Y, Filiz G, Koksalar F et al. MCH Neuron Activity Is Sufficient for Reward and Reinforces Feeding. Neuroendocrinology 2020; 110(3–4): 258–270. [PubMed: 31154452]
65. Noble EE, Hahn JD, Konanur VR, Hsu TM, Page SJ, Cortella AM et al. Control of Feeding Behavior by Cerebral Ventricular Volume Transmission of Melanin-Concentrating Hormone. Cell metabolism 2018; 28(1): 55–68 e57. [PubMed: 29861386]

66. Dackis CA, O'Brien CP. Cocaine dependence: the challenge for pharmacotherapy. Current Opinion in Psychiatry 2002; 15(3): 261–267.

67. Morgan PT, Pace-Schott E, Pittman B, Stickgold R, Malison RT. Normalizing effects of modafinil on sleep in chronic cocaine users. The American journal of psychiatry 2010; 167(3): 331–340. [PubMed: 20080983]

68. Benquet P, Gee CE, Gerber U. Two distinct signaling pathways upregulate NMDA receptor responses via two distinct metabotropic glutamate receptor subtypes. The Journal of neuroscience : the official journal of the Society for Neuroscience 2002; 22(22): 9679–9686. [PubMed: 12427823]

69. Kovalevich J, Corley G, Yen W, Rawls SM, Langford D. Cocaine-induced loss of white matter proteins in the adult mouse nucleus accumbens is attenuated by administration of a beta-lactam antibiotic during cocaine withdrawal. The American journal of pathology 2012; 181(6): 1921–1927. [PubMed: 23031254]

70. Bannon M, Kapatos G, Albertson D. Gene expression profiling in the brains of human cocaine abusers. Addict Biol 2005; 10(1): 119–126. [PubMed: 15849025]

71. Bartzokis G, Beckson M, Lu PH, Edwards N, Bridge P, Mintz J. Brain maturation may be arrested in chronic cocaine addicts. Biological psychiatry 2002; 51(8): 605–611. [PubMed: 11955460]

72. Nielsen DA, Huang W, Hamon SC, Maili L, Witkin BM, Fox RG et al. Forced Abstinence from Cocaine Self-Administration is Associated with DNA Methylation Changes in Myelin Genes in the Corpus Callosum: a Preliminary Study. Front Psychiatry 2012; 3: 60. [PubMed: 22712019]

73. Narayana PA, Ahobila-Vajjula P, Ramu J, Herrera J, Steinberg JL, Moeller FG. Diffusion tensor imaging of cocaine-treated rodents. Psychiatry Res 2009; 171(3): 242–251. [PubMed: 19217266]

74. Navarro AI, Mandyam CD. Protracted abstinence from chronic ethanol exposure alters the structure of neurons and expression of oligodendrocytes and myelin in the medial prefrontal cortex. Neuroscience 2015; 293: 35–44. [PubMed: 25732140]

75. Konadhode RR, Pelluru D, Shiromani PJ. Neurons containing orexin or melanin concentrating hormone reciprocally regulate wake and sleep. Front Syst Neurosci 2014; 8: 244. [PubMed: 25620917]

76. Tsujino N, Sakurai T. Orexin/hypocretin: a neuropeptide at the interface of sleep, energy homeostasis, and reward system. Pharmacol Rev 2009; 61(2): 162–176. [PubMed: 19549926]

77. Torterolo P, Lagos P, Monti JM. Melanin-concentrating hormone: a new sleep factor? Front Neurol 2011; 2: 14. [PubMed: 21516258]

78. Reichelt AC, Westbrook RF, Morris MJ. Integration of reward signalling and appetite regulating peptide systems in the control of food-cue responses. Br J Pharmacol 2015; 172(22): 5225–5238. [PubMed: 26403657]

79. James MH, Stopper CM, Zimmer BA, Koll NE, Bowrey HE, Aston-Jones G. Increased Number and Activity of a Lateral Subpopulation of Hypothalamic Orexin/Hypocretin Neurons Underlies the Expression of an Addicted State in Rats. Biological psychiatry 2019; 85(11): 925–935. [PubMed: 30219208]

80. van den Pol AN. Neuropeptide transmission in brain circuits. Neuron 2012; 76(1): 98–115. [PubMed: 23040809]

81. Svensson E, Apergis-Schoute J, Burnstock G, Nusbaum MP, Parker D, Schioth HB. General Principles of Neuronal Co-transmission: Insights From Multiple Model Systems. Front Neural Circuits 2018; 12: 117. [PubMed: 30728768]

82. Nusbaum MP, Blitz DM, Marder E. Functional consequences of neuropeptide and small-molecule co-transmission. Nat Rev Neurosci 2017; 18(7): 389–403. [PubMed: 28592905]

83. Willie JT, Sinton CM, Maratos-Flier E, Yanagisawa M. Abnormal response of melanin-concentrating hormone deficient mice to fasting: hyperactivity and rapid eye movement sleep suppression. Neuroscience 2008; 156(4): 819–829. [PubMed: 18809470]

84. Izawa S, Chowdhury S, Miyazaki T, Mukai Y, Ono D, Inoue R et al. REM sleep-active MCH neurons are involved in forgetting hippocampus-dependent memories. Science 2019; 365(6459): 1308–1313. [PubMed: 31604241]

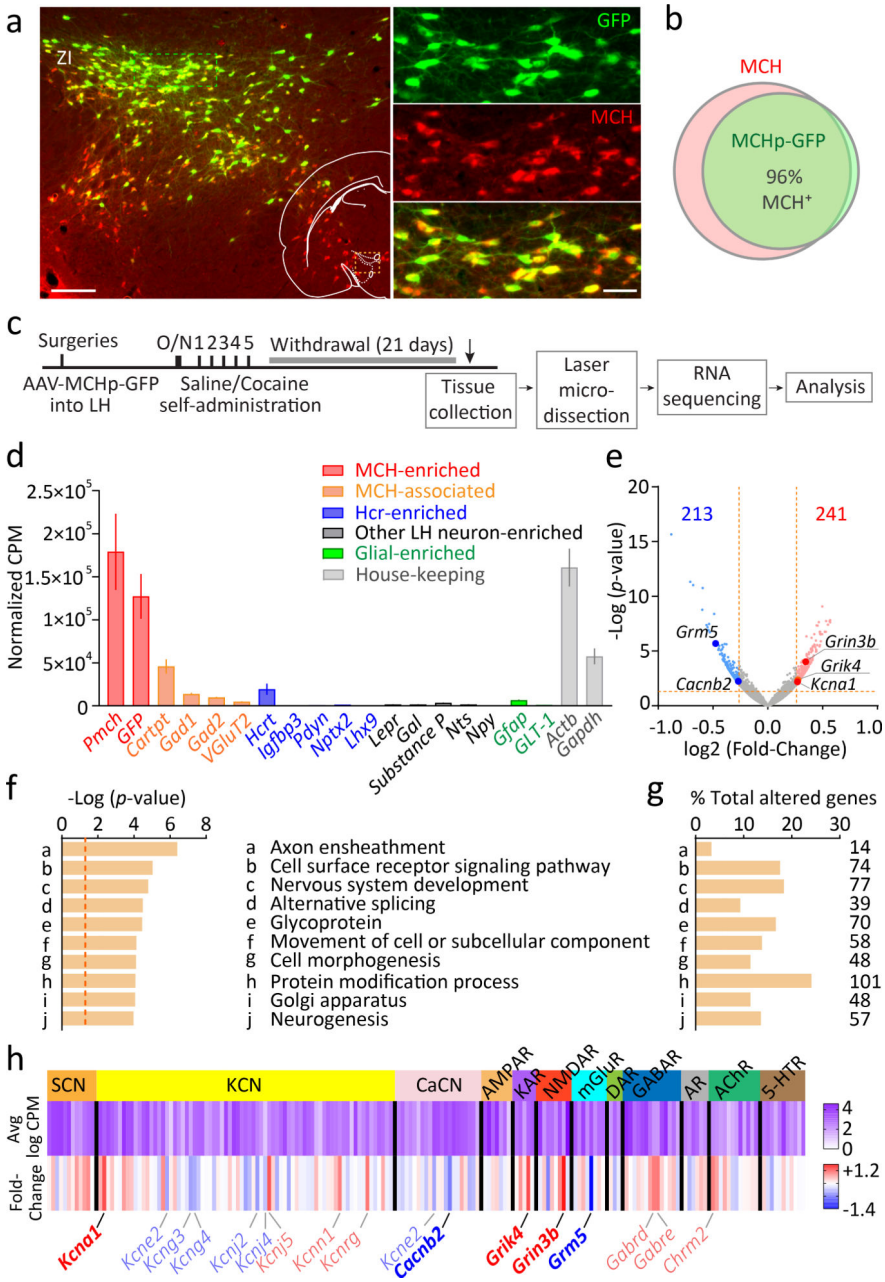

Fig. 1.

Cocaine experience persistently alters gene expression in LH MCH neurons. **a** Example dual-channel fluorescence images showing GFP-labeled LH neurons also exhibited MCH immunoreactivity. ZI, zona incerta. Scale bars = 200 μm, 50 μm. **b** Summary showing ~96% of GFP-labeled cells exhibited MCH immunoreactivity. **c** Timeline of surgery, self-administration of intravenous saline or cocaine training, withdrawal, tissue preparation, and RNA-sequencing. **d** Expression of MCH neuron-enriched, MCH neuron-related, and MCH neuron-non-enriched genes in the sampled cells, demonstrating cell sampling specificity. Data shown as mean ± SEM. CPM = counts per million. **e** Volcano-plot of all 15,585 genes entered for differential expression analysis. Light red indicates genes showing >

20% fold-increase with significant *p* values, and light blue indicates genes showing < −20% fold-decrease with significant *p* values. Among them, genes of interest across voltage-gated ion channels and transmitter receptors are shown in big dots. Orange lines indicate absolute fold-change = 20%, and $p = 0.05$. **f** Top ten significantly altered biological pathway clusters in cocaine- vs. saline-treated rats. *Dotted line*, $p = 0.05$. **g** Number of differentially expressed genes in each functional cluster and % out of total 454 altered genes. **h** Expression profiling of voltage-gated ion channels and neurotransmitter receptors in LH MCH neurons. Average expression of each transcript across all rats is shown as a vertical line with purple intensity positively correlated with level of expression. Fold-change of each transcript is shown as a vertical line with red intensity positively correlated with fold-increase and blue intensity positively correlated with fold-decrease in cocaine-treated rats compared to saline-treated ones. Significant changes in gene expression in cocaine-treated rats are named beneath the heat map with the change in expression color-coded, such that red represents increased expression, and blue indicates decreased expression. Bold fonts indicate genes with absolute fold-change > 20% with significant *p* values compared to saline-treated rats. Light fonts indicate genes with absolute fold-change < 20% with significant *p* values. SCN, voltage-gated sodium channels; KCN, voltage-gated potassium channels; CaCN, voltage-gated calcium channels; AMPAR, AMPA receptors; KAR, kainate receptors; NMDAR, NMDA receptors; mGluR, metabotropic glutamate receptors; DAR, dopamine receptors; GABAR, GABA receptors; AR, adrenergic receptors; AChR, acetylcholine receptors; 5-HTR, serotonin receptors. n = 4 rats each.

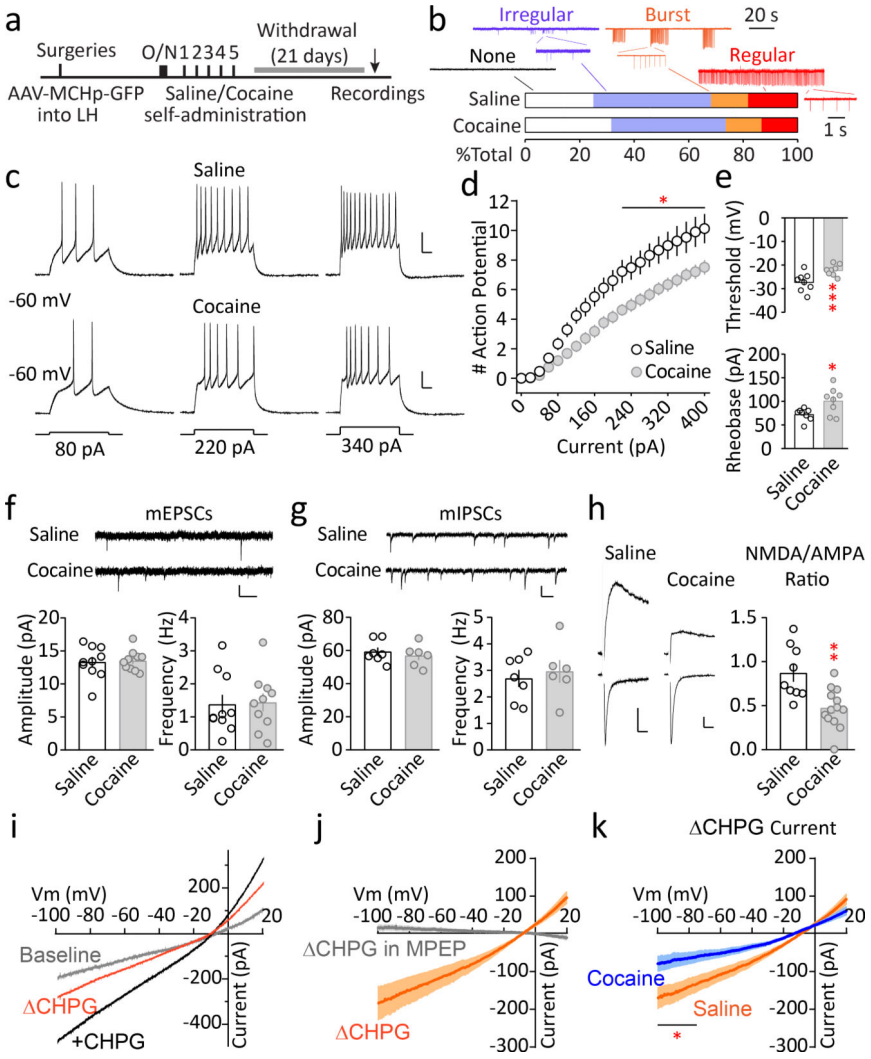

Fig. 2.

Cocaine experience persistently reduces membrane excitability and impairs glutamate receptor activity in LH MCH neurons. **a** Timeline of surgery, self-administration of intravenous saline or cocaine training, withdrawal, and recordings. **b** Example and grouped data showing diverse spontaneous action potential firing patterns and distribution in LH MCH neurons in *in vitro* slices under loose-patch recordings from saline- or cocaine-treated rats after 21 days of withdrawal (n = 44 cells/7 rats and 38 cells/6 rats). **c-d** Example and grouped data showing decreased # of evoked action potentials under stepwise current injections in cocaine-treated rats compared to saline-treated rats (n = 53 or 54 cells/8 rats each), suggesting decreased membrane excitability. Scale bars = 20 mV, 50 ms. **e** The threshold for action potential was more depolarized, and the rheobase current was increased in LH MCH neurons in cocaine-treated rats compared to saline-treated ones (n = 53 or 54 cells/8 rats each). **f-g** Average mEPSCs (**f**) and mIPSCs (**g**) amplitude and frequency were not different between saline- and cocaine-treated rats (**f**, n = 47/10, 45/10; **g**, n = 35/7, 33/6). Scale bars = 20 pA, 200 ms; 50 pA, 200 ms. **h** Example and grouped data showing that the ratio of NMDA/AMPA receptor EPSCs was decreased in cocaine-treated rats (n =

24/9; 39/13). AMPA receptor ESPC peak amplitude was measured at −70 mV, and NMDA receptor EPSC amplitude was operationally defined as the amplitude measured at +40 mV at 35 ms following the peak of AMPA $EPSC_{-70\ mV}$. Scale bars = 20 pA, 10 ms. **i** Example trace of current-voltage relationship of CHPG (100 μM, bath-applied)-induced conductance in LH MCH neurons. **j** blockade of CHPG-induced conductance by the pre-application of MPEP (10 μM) in cocaine-treated rats (n = 8 slices from 3 rats), confirming that the CHPG-induced conductance was mediated by mGluR5 activation. **k** mGluR5 activation-induced current was reduced in cocaine-treated rats (n = 14/6) compared to saline-treated ones (n = 13/6). n = cell number/animal number. Data shown as mean ± SEM. * $p < 0.05$, ** $p < 0.01$

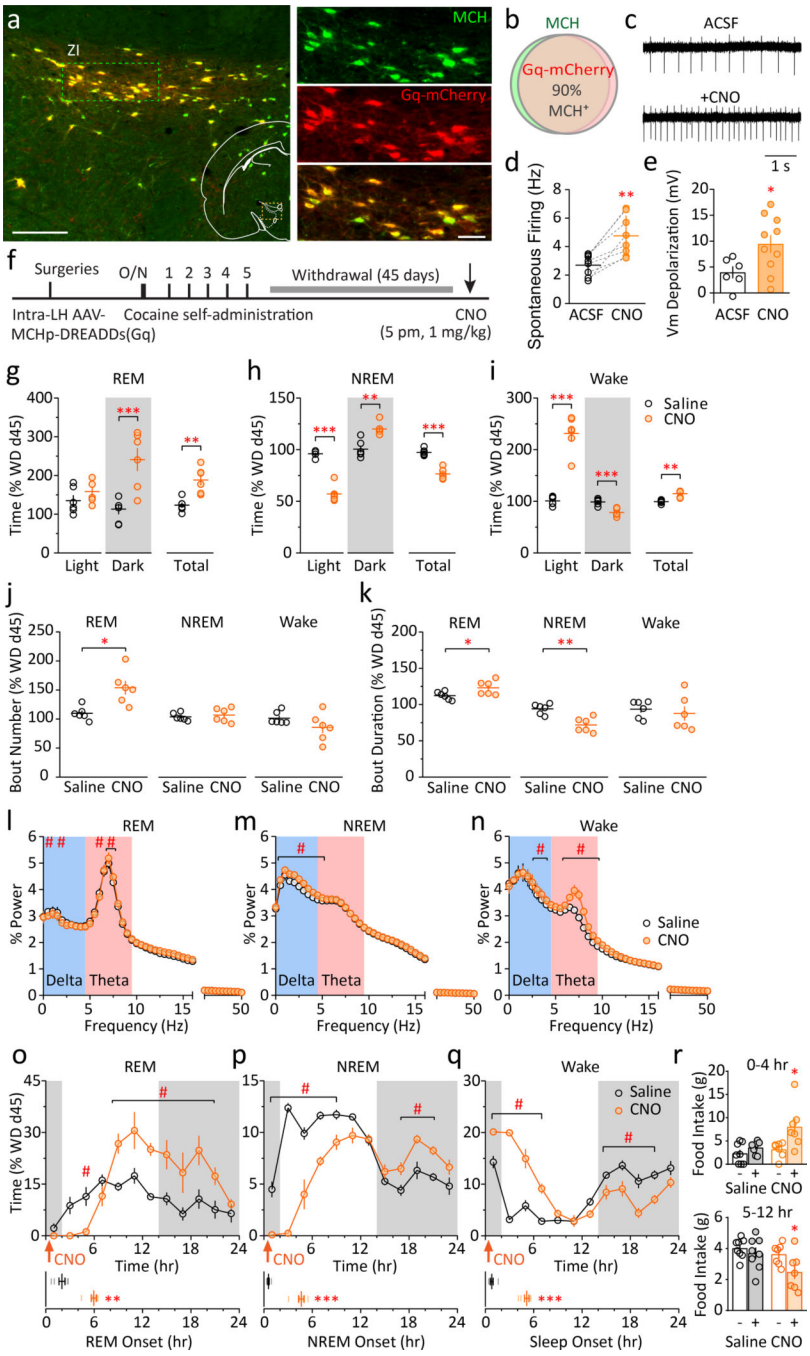

Fig. 3.

Chemogenetic activation of LH MCH neurons during the light (inactive) phase promotes both wakefulness and REM sleep after long-term cocaine withdrawal. **a** Example dual-channel fluorescence images showing mCherry-labeled LH neurons also exhibited MCH immunoreactivity. ZI, zona incerta. Scale bars = 200 μm, 50 μm. **b** Summary showing ~90% of mCherry-labeled cells exhibited MCH immunoreactivity. **c-d** Example and grouped data showing that bath application of CNO (10 μM) increased spontaneous action potential firing frequency in LH MCH neurons in *in vitro* slices under loose-patch recordings (n = 8 slices).

e CNO application depolarized the membrane potential (Vm) in LH MCH neurons (n = 6 or 10 slices). **f** Timeline of surgery, self-administration of intravenous cocaine training, withdrawal, and CNO injection (5 pm, 1 mg/kg). **g-i** Total time of REM sleep (**g**), NREM sleep (**h**), and wakefulness (**i**) across 12-hr light and 12-hr dark (*shaded*) phases and over 24 hrs, following saline or CNO injection, normalized to baseline sleep. **j-k** 24-hr bout analysis showing bout number (**j**) and average bout duration (**k**) changes following saline or CNO injection, normalized to baseline sleep. **l-n** 24-hr power spectrum analysis showing normalized sleep wave power-frequency distribution (0–50 Hz) during REM (**l**), NREM (**m**), and wakefulness (**n**) episodes after saline/CNO injections. Data normalized to 24-hr baseline state average and expressed as %. **o-q** Time spent for REM (**o**), NREM (**p**), and wakefulness (**q**) states every 2 hrs across 12-hr light and 12-hr dark (*shaded*) phases, following saline or CNO injection, normalized to baseline sleep. *Bottom*, REM (first 1-min REM episode), NREM (first 1-min NREM episode), and overall sleep (first 3-min NREM+REM episode) onsets were delayed by CNO injection as compared to saline injection. n = 6 rats each. **r** Food intake was increased during the first 4 hrs after CNO injection, and decreased during the following 8 hrs, as compared to saline injection. n = 8, 7 rats each. Data shown as mean ± SEM. #, * $p < 0.05$, ** $p < 0.01$, *** $p < 0.001$

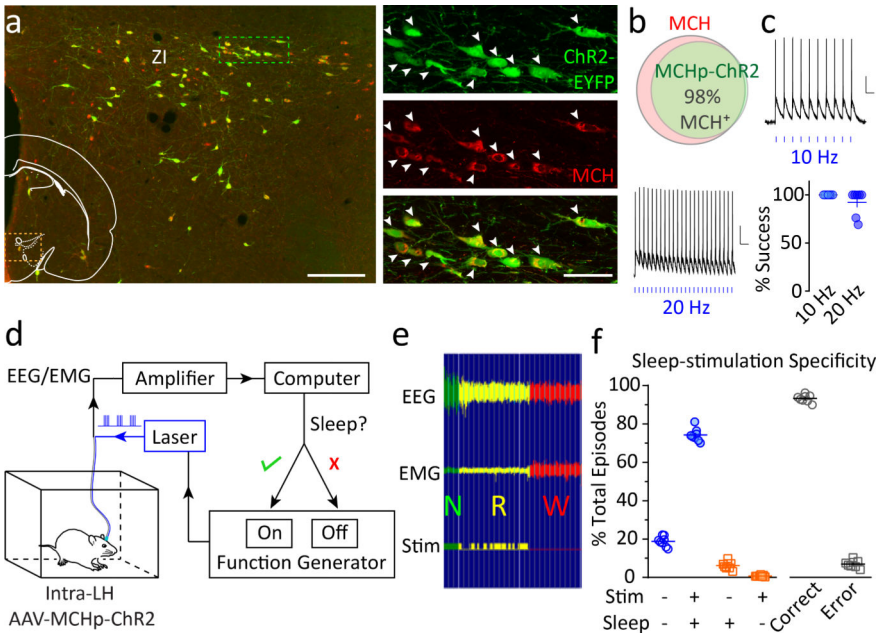

Fig. 4.

In vivo, closed-loop, optogenetic stimulation system for selective stimulation of LH MCH neurons during sleep. **a** Example dual-channel fluorescence images showing EYFP-labeled LH neurons also exhibited MCH immunoreactivity. ZI, zona incerta. Scale bars = 200 μm, 50 μm. **b** Summary showing ~98% of EYFP-labeled cells exhibited MCH immunoreactivity. **c** 473 nm laser stimulation (1 ms pulses) of ChR2-expressing LH MCH neurons evoked high-fidelity action potential firing at 10 and 20 Hz stimulation frequencies. % Success was calculated by % of laser pulses that successfully evoked action potential firing using the 10 Hz or 20 Hz stimulation protocol (1 ms x 10 or 20 Hz, 5 s-ON-5 s-OFF, for 2–5 min). Scale bars = 20 mV, 100 ms. n = 7 cells each. **d** Schematic diagram of the closed-loop, *in vivo* optogenetic stimulation system. **e** Example trace showing sleep-triggered TTL pulse delivery to the function generator during NREM and REM sleep. N: NREM sleep, green; R: REM sleep, yellow; W: wakefulness, red. **f** grouped data showing % of total epochs across 12-hr light phase that were associated with correct or incorrect trigger of TTL pulses (or non-stimulations) from each individual rat, demonstrating high accuracy (93.01 ± 0.67 %; mean ± SEM) of the system in delivering stimulations selectively during sleep. Accuracy was determined by comparing the autoscore-triggered TTL signals against manually scored results in off-line post-analysis. n = 8 rats. Data shown as mean ± SEM.

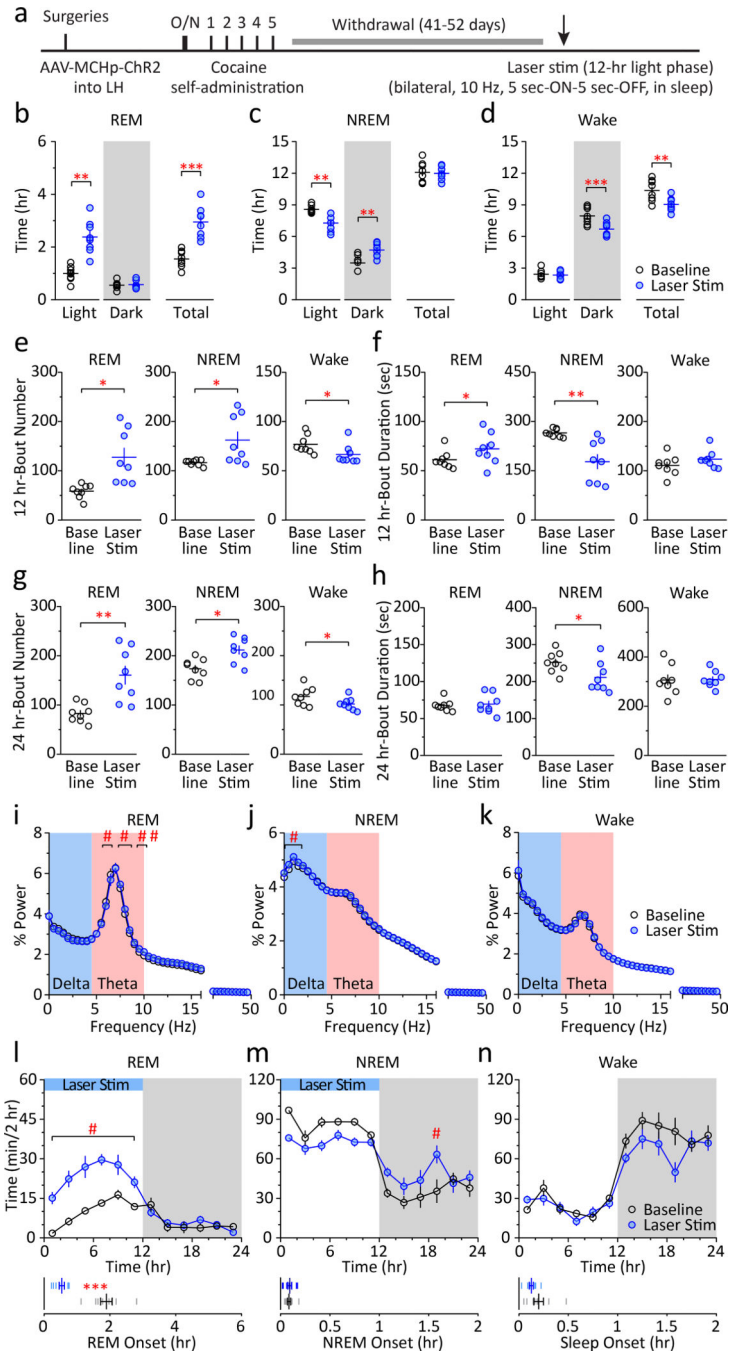

Fig. 5.

Optogenetic activation of LH MCH neurons selectively during sleep increases REM sleep after long-term cocaine withdrawal. **a** Timeline of surgery, self-administration of intravenous cocaine training, withdrawal, and laser stimulation. Laser stimulation was performed on a chosen day after withdrawal day 41–52 to accommodate the availability of the lasers. **b-d** Total time of REM sleep (**b**), NREM sleep (**c**), and wakefulness (**d**) across 12-hr light and 12-hr dark (*shaded*) phases and over 24 hrs, without or with laser stimulation (bilateral, 10 Hz, 5 s-ON-5 s-OFF, in sleep, across 12-hr light phase). **e-f** 12-hr light phase bout

analysis showing bout number (**e**) and average bout duration (**f**) changes following laser stimulation compared to baseline sleep. **g-h** 24-hr bout analysis showing bout number (**g**) and average bout duration (**h**) changes following laser stimulation compared to baseline sleep. **i-k** 24-hr power spectrum analysis showing normalized sleep wave power-frequency distribution during REM (**i**), NREM (**j**), and wakefulness (**k**) epochs upon laser stimulations as compared to baseline sleep. Data normalized to 24-hr baseline state average and expressed as %. **l-n** Time spent for REM (**l**), NREM (**m**), and wakefulness (**n**) states every 2 hrs across 12-hr light and 12-hr dark (*shaded*) phases, without or with laser stimulations. *Bottom*, REM (first 1-min REM episode), NREM (first 1-min NREM episode), and overall sleep (first 3-min sleep episode) onsets upon laser stimulations as compared to baseline sleep. n = 8 rats each. Data shown as mean ± SEM. #, * $p < 0.05$, ** $p < 0.01$, *** $p < 0.001$